Journal of Mathematical Research with Applications
Jan., 2017, Vol. 37, No. 1, pp. 1–18
DOI:10.3770/j.issn:2095-2651.2017.01.001
Http://jmre.dlut.edu.cn

Numerical Solution of a Scalar One-Dimensional Monotonicity-Preserving Nonlocal Nonlinear Conservation Law

Qiang DU[1,*], **Zhan HUANG**[2]

1. *Department of Applied Physics and Applied Mathematics, Columbia University, New York, NY* 10027, *USA*
2. *Department of Mathematics, Penn State University, University Park, PA* 16802, *USA*

Dedicated to Professor Renhong WANG on the Occasion of His Eightieth Birthday

Abstract In this paper, we present numerical studies of a recently proposed scalar nonlocal nonlinear conservation law in one space dimension. The nonlocal model accounts for nonlocal interactions over a finite horizon and enjoys maximum principle, monotonicity-preserving and entropy condition on the continuum level. Moreover, it has a well-defined local limit given by a conventional local conservation laws in the form of partial differential equations. We discuss convergent numerical approximations that preserve similar properties on the discrete level. We also present numerical experiments to study various limiting behavior of the numerical solutions.

Keywords nonlocal model; nonlinear hyperbolic conservation laws; maximum principle; monotonicity preserving; numerical solution

MR(2010) Subject Classification 35L65; 45G10

1. Introduction

Recently, a scalar nonlocal nonlinear hyperbolic conservations laws of the form:

$$\begin{aligned} &\frac{\partial u}{\partial t}+\int_0^\delta \Big(\frac{g(u,\tau_h u)-g(\tau_{-h}u,u)}{h}\Big)\omega^\delta(h)\mathrm{d}h=0, \quad (x,t)\in\mathbb{R}\times[0,T],\\ &u(x,0)=u_0(x), \quad x\in\mathbb{R} \end{aligned} \tag{1.1}$$

has been proposed in [1]. Here, the parameter $\delta>0$ is called the nonlocal "horizon" which measures the range of nonlocal interactions. The kernel function $\omega^\delta=\omega^\delta(s)$ is assumed to be symmetric $\omega^\delta(-s)=\omega^\delta(s)$, nonnegative $\omega^\delta(s)\geq 0$, integrable $\omega^\delta\in L^1(\mathbb{R})$, and with its support in the interval $[-\delta,\delta]$. $\tau_{\pm h}u(x,t)=u(x\pm h,t)$ denote shift operations and u_0 is the initial data. The two-point flux $g=g(u_1,u_2)$ is assumed to satisfy the conditions specified later.

Equation (1.1) is spatially "nonlocal", in contrast to its local limit given by the classical

Received December 5, 2016; Accepted December 19, 2016
Supported in part by the NSF (Grant No. DMS-1558744), the AFOSR MURI Center for Material Failure Prediction Through Peridynamics and the ARO MURI (Grant No. W911NF-15-1-0562).
* Corresponding author
E-mail address: qd2125@columbia.edu (Qiang DU); zxh117@psu.edu (Zhan HUANG)

scalar one-dimensional hyperbolic conservation law

$$\begin{aligned} &u_t + \partial_x f(u) = 0, \quad (x,t) \in \mathbb{R} \times [0,T], \\ &u(x,0) = u_0(x), \quad x \in \mathbb{R}, \end{aligned} \tag{1.2}$$

where $f(u) = g(u,u)$ is the local flux function. As noted in [1], formally, equation (1.1) may be seen as a continuum average of the three-point conservative finite difference scheme of (1.2) given by:

$$u_j^{n+1} - u_j^n + \frac{\Delta t}{\Delta x}[g(u_j^n, u_{j+1}^n) - g(u_{j-1}^n, u_j^n)] = 0, \tag{1.3}$$

with the two-point flux function $g = g(u,v)$. For (1.2) and (1.3), it is well known that if $g = g(u,v)$ is monotone, i.e., non-decreasing in u and non-increasing in v, then the scheme (1.3) is monotone, and hence is total-variation-stable (TVS) and enjoys the maximum principle at the discrete level [2,3]. By picking appropriate g with such properties, numerical solutions of scheme (1.3) converge to the unique entropy solution of the local conservation law (1.2) with increased numerical resolution.

For motivations of our interests in (1.1), we note that nonlocality has been introduced in various ways in the modeling of diffusive and convective processed in the past, see [1] for additional background and references. Earlier attempts have been made to generalize local conservations laws in the form of PDEs to the nonlocal setting such as [4–16]. Other studies of nonlocal models can be found in [17,18].

Considering nonlocal interactions with a finite range, one can find studies of models with convective effects in [19] and [20] in the linear case and [21] on nonlinear models. For the nonlinear model in [21], only local existence results are established due to the lack of maximum principle. In [1], a new formulation is proposed to replace the model given in [21] so that maximum principle and monotonicity-preserving properties can be preserved. The entropy condition also follows as a consequence. Moreover, the existence and uniqueness of weak solutions of (1.1) have been successfully established in [1] without assuming a priori bounds on the solutions. The nonlocal Burgers equation studied in [5,16] has a different form but it also allows finite range interactions by using a convective velocity given in terms of the convolution with a compactly supported kernel. In general, unlike the model studied in this work, the nonlocal form presented in [5,16] does not satisfy the entropy condition automatically on the continuum level. As pointed out in [1], for a quadratic nonlinear flux, both the models in [21] and in this paper can also be formulated in the form of a nonlocal flux but with more general kernels G that are no longer translation invariant. Furthermore, the particular nonlocal conservation laws studied here may be viewed as more physical continuum models as they preserve the unwinding feature and the classical entropy conditions on the continuum level.

In this work, we carry out further numerical studies of (1.1). The numerical method we employ is a monotone scheme that has been used in [1] to prove the well-posedness of (1.1). Such a scheme shares much of the monotone schemes for local conservations laws, that is, it satisfies maximum principle, monotonicity-preserving and total-variation-stable, so that numerical solutions are convergent to the continuum solution which automatically satisfies the entropy

condition. We also show that a nonlocal Lax-Friedrich's scheme can be reformulated within the same class of schemes. In our numerical experiments, we take g as the numerical flux of finite difference scheme for local Burgers' equation, so that our nonlocal conservation law can be seen as a "nonlocal Burgers' equation". We perform several types of experiments for the nonlocal scheme using different initial data u_0 and kernels ω^δ, as specified below:

(i) for a fixed δ, refining Δx and Δt;

(ii) for fixed Δx and Δt, refining δ;

(iii) for a fixed number of interaction cells, $r = \lfloor \delta/\Delta x \rfloor$, refining δ (hence Δx and Δt simultaneously);

From these runs, we get to examine the convergence of numerical approximations in different regimes and the behavior of solutions to the nonlocal model.

1.1. Some basic definitions and properties of nonlocal models

We first recall some basic elements of the new nonlocal model and the relevant discrete schemes, as presented in [1].

2. Model specification and properties

For the nonlocal conservation law, the nonlocal interaction kernel $\omega^\delta : \mathbb{R} \to [0, +\infty)$ is a nonnegative density, supported in $(0, \delta)$. That is,

$$\omega^\delta \geq 0, \quad \omega^\delta \text{ is supported on } [0, \delta], \quad \int_0^\delta \omega^\delta(h)\mathrm{d}h = 1. \tag{2.1}$$

It can be taken as $\omega^\delta(h) = \frac{1}{\delta}\rho(\frac{h}{\delta})$, where ρ is a non-negative density function supported on $[0, 1]$. In this paper we assume that $\omega^\delta \in C^2(0, \delta)$.

For convenience we sometimes omit the dependence on δ, and abbreviate ω^δ as ω, $u(x, t)$ as $u(x)$ and the partial derivative of g with respect to the first or second argument as g_i $(i = 1, 2)$. Let $\Omega \subset \mathbb{R}$ be a bounded domain and T be a finite terminal time.

The flux g in (1.1) may take on different forms. But independent of the special choices, it is assumed to have the following properties.

(i) g is consistent with a local flux f:

$$g(u, u) = f(u). \tag{2.2}$$

(ii) $g : W^{1,\infty}(\mathbb{R}) \times W^{1,\infty}(\mathbb{R}) \to W^{1,\infty}(\mathbb{R})$ and its partial derivatives, denoted as g_1 and g_2, are Lipschitz continuous, with Lipschitz constant C:

$$||g(a, b) - g(c, d)||_\infty + \sum_{i=1}^{2} ||g_i(a, b) - g_i(c, d)||_\infty \leq C(||a - c||_\infty + ||b - d||_\infty). \tag{2.3}$$

(iii) g is nondecreasing with respect to the first argument, and nonincreasing to the second argument:

$$g_1(u_1, u_2) := \frac{\partial g}{\partial u_1}(u_1, u_2) \geq 0, \quad g_2(u_1, u_2) := \frac{\partial g}{\partial u_2}(u_1, u_2) \leq 0. \tag{2.4}$$

(iv) Partial derivatives $\{g_i\}$ are bounded in $L^\infty(\mathbb{R})$,

$$||g_i(a,b)||_\infty \le C(||a||_\infty + ||b||_\infty), \quad i = 1, 2, \tag{2.5}$$

where the constant C only depends on g. Classical examples for the construction of such a flux function include Godunov's scheme [22] and Lax-Friedrich's scheme.

Some useful notions of numerical schemes for local conservation laws have been developed in the literature. They are equally applicable to the nonlocal conservation laws at the continuum level. We list a few of them below:

- Conservative: a scheme for (1.2) is conservative, if it is of the form (1.3).
- Consistent: a scheme like (1.3) is consistent if g satisfies $g(u,u) = f(u)$.
- Monotone: a scheme is monotone if

$$u_j^n \le v_j^n \quad \text{for all } n, j. \tag{2.6}$$

- Total-variation-diminishing (TVD), if we have

$$\sum_j |u_{j+1}^{n+1} - u_j^{n+1}| \le \sum_j |u_{j+1}^n - u_j^n|, \tag{2.7}$$

- Maximum principle preserving, if

$$\min_k u_k^0 \le u_j^n \le \max_k u_k^0, \quad \text{for all } n, j. \tag{2.8}$$

We can get a conservative monotone scheme by picking g to be monotone, i.e., non-decreasing on the first argument, and non-increasing on the second argument. The usual CFL condition

$$\frac{\Delta t}{\Delta x}\big(|\frac{\partial g(a,b)}{\partial a}| + |\frac{\partial g(a,b)}{\partial b}|\big) \le 1, \tag{2.9}$$

is needed. The scheme is then automatically monotonicity preserving, TVD and maximum principle preserving [3]. The nonlocal model studied here shares many of the above properties which are also consistent to the physical intuition. In particular, the nonlocal conservation law (1.1) enjoys the maximum principle, that is, if u obtains its maximum and minimum in $U_T = \overline{\Omega} \times [0,T]$, then $\Gamma_T = (\partial\Omega \times (0,T]) \cup (\bar{\Omega} \times \{t = 0\})$, we have

$$\max_{U_T} u = \max_{\Gamma_T} u, \quad \min_{U_T} u = \min_{\Gamma_T} u.$$

Moreover, it has been shown in [1] that a nonlocal entropy condition is automatically satisfied by the solution of (1.1), that is, the following Kružkov-type entropy inequality is satisfied:

$$\int_0^T \int_{\mathbb{R}} |u - c|\phi_t \mathrm{d}x\mathrm{d}t + \int_0^T \int_{\mathbb{R}} \int_0^\delta \frac{\tau_h\phi - \phi}{h} q(u, \tau_h u)\omega(h)\mathrm{d}h\mathrm{d}x\mathrm{d}t \ge 0 \tag{2.10}$$

for $\phi \in C_0^1(\mathbb{R} \times [0,T])$ with $\phi \ge 0$ and any constant $c \in \mathbb{R}$. Here, q is the nonlocal entropy flux corresponding to the entropy function $\eta(u,c) = |u - c|$, defined as

$$q(a,b;c) = g(a \vee c, b \vee c) - g(a \wedge c, b \wedge c), \tag{2.11}$$

or equivalently,

$$q(a,b;c) = \mathrm{sgn}(b-a)\big\{\frac{\mathrm{sgn}(a-c) + \mathrm{sgn}(b-c)}{2}[g(a,b) - g(c,c)] +$$

$$\frac{\mathrm{sgn}(a-c)-\mathrm{sgn}(b-c)}{2}[g(c,b)-g(a,c)]\big\},$$

where $\mathrm{sgn}(0)=1$. In particular, by the consistency of g stated in (2.2), we have

$$q(u,u;c)=g(u\vee c,u\vee c)-g(u\wedge c,u\wedge c)=\mathrm{sgn}(u-c)[f(u)-f(c)]=\mathrm{q}(u,c),$$

where $\mathrm{q}(u,c)$ is the local entropy flux. The inequality (2.10) is referred to as the entropy inequality for the nonlocal conservation law (1.1).

2.1. Localization of the nonlocal conservation law

A key feature of our nonlocal model is the explicit use of the nonlocal horizon parameter δ to characterize the range of nonlocal interactions. This is inspired by the same notion used in peridynamics [23,24]. Mathematical studies associated with the limit $\delta\to 0$ have been discussed extensively, see [25–28]. We now show formally that the nonlocal conservation law (1.1) reduces to the local one (1.2). We denote $\bar{\delta}$ as the Dirac delta function.

Lemma 2.1 *Assume $g\in C^1(\mathbb{R}\times\mathbb{R})$, $u\in C^1(\mathbb{R})$, and that*

$$\lim_{\delta\to 0}\omega^\delta(h)\to\bar{\delta}(h) \tag{2.12}$$

in the distribution sense. Then:

$$\lim_{\delta\to 0}\int_0^\delta [g(u(x),u(x+h))-g(u(x-h),u(x))]\frac{\omega^\delta(h)}{h}\mathrm{d}h=[f(u)]_x.$$

Proof By assumption, for any (x,t), $\frac{g(u(x),u(x+h))-g(u(x-h),u(x))}{h}$, as a function of h, is in $C^1(\mathbb{R})$. By (2.12), we have

$$\begin{aligned}
&\lim_{\delta\to 0}\int_{\mathbb{R}}\frac{g(u(x),u(x+h))-g(u(x-h),u(x))}{h}\omega^\delta(h)\mathrm{d}h\\
&=\int_{\mathbb{R}}\frac{g(u(x),u(x+h))-g(u(x-h),u(x))}{h}\bar{\delta}(h)\mathrm{d}h\\
&=\lim_{h\to 0}\frac{g(u(x),u(x+h))-g(u(x-h),u(x))}{h}\\
&=\lim_{h\to 0}\frac{g(u(x),u(x+h))-g(u(x),u(x))}{u(x+h)-u(x)}\big(\frac{u(x+h)-u(x)}{h}\big)+\\
&\quad\lim_{h\to 0}\frac{g(u(x),u(x))-g(u(x-h),u(x))}{u(x)-u(x-h)}\big(\frac{u(x)-u(x-h)}{h}\big)\\
&=g_2(u(x),u(x))u'(x)+g_1(u(x),u(x))u'(x)=[g(u,u)]_x=[f(u)]_x.
\end{aligned}$$

The last equality comes from the consistency of g with local flux f (2.2). □

The next lemma shows that if there is a function u, in the suitable function space, satisfying a nonlocal entropy condition, then as $\delta\to 0$, u also satisfies local entropy condition.

Lemma 2.2 *Assume that g satisfies (2.2), (2.3) and (2.4), and kernel ω^δ satisfies condition (2.1). Let $u\in L^\infty(\mathbb{R}\times\mathbb{R}^+)$, $u(\cdot,t)\in BV(\mathbb{R})$ for any $t\in[0,T]$, and u satisfies the nonlocal entropy inequality. Then as $\delta\to 0$, u also satisfies the local entropy inequality (2.13), that is,*

for any $\phi \in C_0^1(\mathbb{R}\times(0,T))$ *with* $\phi \geq 0$ *and any* $c \in \mathbb{R}$,

$$\int_0^T \int_{\mathbb{R}} |u-c|\phi_t + \mathrm{sgn}(u-c)(f(u)-f(c))\partial_x \psi \mathrm{d}x\mathrm{d}t \geq 0. \tag{2.13}$$

Proof Since u satisfies the nonlocal entropy inequality (2.10), we have

$$\int_0^T \int_{\mathbb{R}} \phi_t |u-c| \mathrm{d}x\mathrm{d}t + \int_0^T \int_{\mathbb{R}} \int_0^\delta \frac{\tau_h\phi - \phi}{h} q(u,\tau_h u)\omega^\delta(h)\mathrm{d}h\mathrm{d}x\mathrm{d}t \geq 0.$$

Recall that $q(u,u) = \mathrm{sgn}(u-c)(f(u)-f(c))$, we only need to prove

$$\lim_{\delta\to 0}\int_0^T \int_{\mathbb{R}} \int_0^\delta \frac{\tau_h\phi-\phi}{h} q(u,\tau_h u)\omega^\delta(h)\mathrm{d}h\mathrm{d}x\mathrm{d}t = \int_0^T\int_{\mathbb{R}} \partial_x(\phi(x))q(u,u)\mathrm{d}x\mathrm{d}t.$$

Let us suppose that the compact support of ϕ is in $[a,b]\times[0,T]$. By boundedness of q and the fact that $\omega^\delta \in L^1(\mathbb{R})$ (2.1), we have

$$\begin{aligned}
&\Big|\int_0^\delta \frac{\tau_h\phi-\phi}{h} q(u,\tau_h u)\omega^\delta(h)\mathrm{d}h\Big| \leq \int_0^\delta C||\phi_x||_{L^\infty(\mathbb{R})}(||u||_{L^\infty(\mathbb{R})}+1)\omega^\delta(h)\mathrm{d}h\\
&\leq C\int_0^\delta \omega^\delta(h)\mathrm{d}h \leq C,
\end{aligned}$$

so we can apply the dominated convergence theorem to get

$$\begin{aligned}
&\lim_{\delta\to 0}\int_0^T\int_{\mathbb{R}}\int_0^\delta [\phi(x+h,t)-\phi(x,t)]q(u,\tau_h u)\frac{\omega^\delta(h)}{h}\mathrm{d}h\mathrm{d}x\mathrm{d}t\\
&= \lim_{\delta\to 0}\int_0^T\int_a^b\int_0^\delta [\phi(x+h,t)-\phi(x,t)]q(u,\tau_h u)\frac{\omega^\delta(h)}{h}\mathrm{d}h\mathrm{d}x\mathrm{d}t\\
&= \int_0^T\int_a^b \Big(\lim_{\delta\to 0}\int_0^\delta [\phi(x+h,t)-\phi(x,t)]q(u,\tau_h u)\frac{\omega^\delta(h)}{h}\mathrm{d}h\Big)\mathrm{d}x\mathrm{d}t\\
&= \int_0^T\int_a^b \partial_x(\phi(x))q(u,u)\mathrm{d}x\mathrm{d}t,
\end{aligned}$$

where the last equality is based on the following fact

$$\lim_{\delta\to 0}\int_0^\delta [\phi(x+h,t)-\phi(x,t)]q(u,\tau_h u)\frac{\omega^\delta(h)}{h}\mathrm{d}h = \partial_x(\phi(x))q(u,u), \tag{2.14}$$

for (x,t) almost everywhere in $[a,b]\times[0,T]$, which is to be proved next.

In fact, for any $t\in[0,T]$, since $u(\cdot,t)$ is a BV function, $u(\cdot,t)$ is continuous with respect to x almost everywhere on $\mathbb{R}$. Let $x\in[a,b]$ be a continuity point of $u(\cdot,t)$. Then for any $\varepsilon>0$, there exists a $\delta^*>0$, such that for any $\delta<\delta^*$,

$$\Big|\frac{\phi(x+h)-\phi(x)}{h}-\phi_x\Big| \leq \varepsilon,\ |u(x)-u(x+h)|\leq\varepsilon,\quad \text{a.e } h\in(0,\delta].$$

So by the boundedness and Lipschitz continuity of q, we have

$$\begin{aligned}
&\Big|\frac{\phi(x+h)-\phi(x)}{h}q(u,\tau_h u)-\phi_x q(u,u)\Big|\\
&\leq \Big|\frac{\phi(x+h)-\phi(x)}{h}-\phi_x\Big|\cdot|q(u,\tau_h u)| + |\phi_x|\cdot|q(u,\tau_h u)-q(u,u)|\\
&\leq \Big|\frac{\phi(x+h)-\phi(x)}{h}-\phi_x\Big|C(||u||_{L^\infty(\mathbb{R})}+1)+C|u-\tau_h u| \leq C\varepsilon,
\end{aligned}$$

with $C = C(\phi, ||u||_{L^\infty}, g)$. Therefore,

$$\begin{aligned}
&\Big| \int_0^\delta \frac{\phi(x+h)-\phi(x)}{h} q(u, \tau_h u)\omega^\delta(h)\mathrm{d}h - \phi_x q(u,u)\Big| \\
&\le \Big| \int_0^\delta \frac{\phi(x+h)-\phi(x)}{h} q(u, \tau_h u)\omega^\delta(h)\mathrm{d}h - \int_0^\delta \phi_x q(u,u)\omega^\delta(h)\mathrm{d}h\Big| \\
&\le \int_0^\delta \Big|\frac{\phi(x+h)-\phi(x)}{h} q(u, \tau_h u) - \phi_x q(u,u)\Big|\omega^\delta(h)\mathrm{d}h \\
&\le C\varepsilon \int_0^\delta \omega^\delta(h)\mathrm{d}h = C\varepsilon,
\end{aligned}$$

where $C = C(\phi, ||u||_{L^\infty}, g)$, which gives (2.14) and thus completes the proof. □

At least formally, we can see from the above discussion the close connection between the nonlocal models and their local limits as $\delta \to 0$ with nonlocal interaction kernels getting localized. Thus, nonlocal models may be viewed as natural generalizations of their local counterpart. For a more rigorous theory on the convergence of the weak solutions, we refer to [1].

3. Numerical schemes for nonlocal models and their local limits

In [1], a monotone scheme was proposed for discretizing the nonlocal conservation law (1.1). Denote Δx and Δt as the spacial and time grid-size, $\mathcal{I}_j = [(j-\frac{1}{2})\Delta x, (j+\frac{1}{2})\Delta x)$ and $\mathcal{I}^n = [n\Delta t, (n+1)\Delta t)$ as the spacial and time cells, and grid points x^n, t^n as the mid-point of $\mathcal{I}_j$ and $\mathcal{I}^n$. Denote u_j^n as the numerical solution at grid point (x_j, t^n). In this work, for simplicity, we always take the grid size $\Delta h = \Delta x$. We pay close attention to the notion of asymptotic compatibility developed in [27,29] for the discretization of nonlocal models. Such a property is important for validation and verification as it ensures that the discrete numerical solutions of the nonlocal model can give the correct limit as the mesh gets refined and the nonlocal horizon shrinks.

Let us fix $(x,t) = x_j, t^n$ and consider the following forward-in-time conservative scheme for the nonlocal problem (1.1):

$$\begin{cases} \dfrac{u_j^{n+1}-u_j^n}{\Delta t} + \displaystyle\sum_{k=1}^{r\vee 1} [g_{j,j+k} - g_{j-k,j}]W_k = 0, \\ u_j^0 = \dfrac{1}{\Delta x}\displaystyle\int_{\mathcal{I}_j} u_0(x)\mathrm{d}x, \end{cases} \tag{3.1}$$

where $\mathcal{I}_j := [x_{j-\frac{1}{2}}, x_{j+\frac{1}{2}})$, $g_{i,j} := g(u_i, u_j)$ and for $k \le r$,

$$W_k = \begin{cases} \dfrac{1}{k\Delta x}\displaystyle\int_{(k-1)\Delta x}^{k\Delta x} \omega^\delta(h)\mathrm{d}h + \dfrac{\mathbf{1}_{k=r}}{r\Delta x}\displaystyle\int_{r\Delta x}^{\delta} \omega^\delta(h)\mathrm{d}h, & r \ge 2, \\ \dfrac{1}{\Delta x}, & r = 1. \end{cases} \tag{3.2}$$

Here $\mathbf{1}_{m=n}$ is the Kronecker-Delta that gives value 1 for $m = n$ and 0 for $m \ne n$.

Remark 3.1 Since ω satisfies (2.1), W_k defined in (3.2) satisfies

$$\Delta x \sum_{k=1}^{r\vee 1} kW_k = 1, \quad \text{for any pair } (\Delta x, \delta). \tag{3.3}$$

Equivalently, we may reformulate the first equation in (3.1) as

$$u_j^{n+1} = H(u_{j-r}^n, \ldots, u_j^n, \ldots, u_{j+r}^n) \tag{3.4}$$

with H defined as

$$H(u_{j-r}^n, \ldots, u_j^n, \ldots, u_{j+r}^n) = u_j^n - \Delta t \sum_{k=1}^{r\vee 1} [g_{j,j+k} - g_{j-k,j}]W_k. \tag{3.5}$$

In the following, we refer scheme (3.1) or (3.4) as the nonlocal scheme for convenience.

Remark 3.2 If we fix spacial mesh Δx, let $\delta < \Delta x$ and $\delta \to 0$, the first equation in scheme (3.1) reduces to

$$u_j^{n+1} = u_j^n - \frac{\Delta t}{\Delta x}[g(u_j, u_{j+1}) - g(u_{j-1}, u_j)], \tag{3.6}$$

which is a standard finite difference scheme for local conservation law (1.2), where g serves as the numerical flux function.

Like the local case, we note that a nonlocal version of Lax-Friedrich's scheme can also be seen as the forward-in-time scheme (3.1) with a new flux $\tilde{g}$. Indeed, consider the following "nonlocal" Lax-Friedrich's scheme

$$\frac{u_j^{n+1} - \frac{1}{2}\sum_{k=1}^{r\vee 1} Q_k^r (u_{j+k}^n + u_{j-k}^n)}{\Delta t} + \sum_{k=1}^{r\vee 1} [g_{j,j+k} - g_{j-k,j}]W_k = 0. \tag{3.7}$$

The coefficients $\{Q_k^r\}_k$ may depend on r, and are required to satisfy the following conditions:

$$\sum_{k=1}^{r\vee 1} Q_k^r = 1, \quad Q_k^r \geq 0, \quad \sup_{r\geq 1} \sum_{k=1}^{r} Q_k^r k^2 < \infty. \tag{3.8}$$

Remark 3.3 An example of Q_k^r is:

$$Q_k^r = \frac{C_r}{k^4}, \quad C_r = \Big(\sum_{k=1}^{r} \frac{1}{k^4}\Big)^{-1}. \tag{3.9}$$

Note that the case $Q_k^r \equiv C$ (with C being a constant independent of k) violates the third condition in (3.8). When $r = 1$, $Q_k^r = 1$, it recovers the classical Lax-Friedrich's method: $\frac{u_j^{n+1} - \frac{1}{2}(u_{j+1}^n + u_{j-1}^n)}{\Delta t} \sim u_t$.

Lemma 3.4 *Assume that $\{Q_k^r\}_k$ satisfies the second condition in (3.8). Taking*

$$Q_k^r = \Delta x(kW_k), \tag{3.10}$$

then, the first condition in (3.8) is automatically satisfied due to (3.3), and the nonlocal Lax-Friedrich's scheme (3.7) can be written into the form of forward-in-time scheme (3.1), with a new flux

$$\tilde{g}(u_j, u_{j+k}) = g(u_j, u_{j+k}) - \frac{k}{2\beta}(u_{j+k} - u_j), \quad \text{where } \beta = \frac{\Delta t}{\Delta x}. \tag{3.11}$$

Moreover, if g satisfies conditions (2.2)–(2.5), so does $\tilde{g}$.

Proof The nonlocal Lax-Friedrich's scheme (3.7) can be rewritten as

$$\frac{u_j^{n+1}-u_j^n}{\Delta t}=\frac{1}{\Delta t}\Big[\frac{1}{2}\sum_{k=1}^{r\vee 1}Q_k^r(u_{j+k}^n+u_{j-k}^n)-u_j^n\Big]-\sum_{k=1}^{r}[g_{j,j+k}-g_{j-k,j}]W_k.$$

Note that, by the first condition on Q_k^r in (3.8),

$$\begin{aligned}\frac{1}{2}\sum_{k=1}^{r\vee 1}Q_k^r(u_{j+k}^n+u_{j-k}^n)-u_j^n&=\frac{1}{2}\sum_{k=1}^{r\vee 1}Q_k^r(u_{j+k}^n+u_{j-k}^n)-\Big(\sum_{k=1}^{r\vee 1}Q_k^r\Big)u_j^n\\&=\frac{1}{2}\sum_{k=1}^{r\vee 1}Q_k^r[(u_{j+k}^n-u_j^n)-(u_j^n-u_{j-k}^n)].\end{aligned}$$

Plugging it in and using the definition of Q_k^r in (3.10) and the notation $g_{j,k}^n=g(u_j^n,u_k^n)$, one has

$$\begin{aligned}\frac{u_j^{n+1}-u_j^n}{\Delta t}&=\sum_{k=1}^{r\vee 1}\Big\{\frac{Q_k^r}{2\Delta t}[(u_{j+k}^n-u_j^n)-(u_j^n-u_{j-k}^n)]-W_k(g_{j,j+k}^n-g_{j-k,j}^n)\Big\}\\&=\sum_{k=1}^{r\vee 1}\frac{Q_k^r}{k\Delta x}\frac{k}{2\beta}[(u_{j+k}^n-u_j^n)-(u_j^n-u_{j-k}^n)]-\sum_{k=1}^{r\vee 1}W_k(g_{j,j+k}^n-g_{j-k,j}^n)\\&=\sum_{k=1}^{r\vee 1}W_k\Big\{\frac{k}{2\beta}(u_{j+k}^n-u_j^n)-\frac{k}{2\beta}(u_j^n-u_{j-k}^n)-(g_{j,j+k}^n-g_{j-k,j}^n)\Big\}\\&=-\sum_{k=1}^{r\vee 1}W_k[\tilde{g}(u_j^n,u_{j+k}^n)-\tilde{g}(u_{j-k}^n,u_j^n)]\end{aligned}$$

where in the last equality, the new flux $\tilde{g}$ is taken as

$$\tilde{g}(u_j^n,u_{j+k}^n)=g_{j,j+k}^n-\frac{k}{2\beta}(u_{j+k}^n-u_j^n).$$

Moreover, it is easy to verifty (2.2–2.5) for $\tilde{g}$ whenever the same equations hold for g.

Under the assumption that Δx and Δt satisfy the CFL condition:

$$(\frac{\Delta t}{\Delta x})\big(\sup_{B_1\le a,b\le B_2}|g_1(a,b)|+\sup_{B_1\le a,b\le B_2}|g_2(a,b)|\big)\le 1, \tag{3.12}$$

the convergence of the numerical scheme has been established in [1]. Specifically, let u_j^n be the numerical solution of scheme (3.1). Denote $\mathcal{I}_j=[(j-\frac{1}{2})\Delta x,(j+\frac{1}{2})\Delta x)$, and $\mathcal{I}^n=[n\Delta t,(n+1)\Delta t)$. Define piecewise constant function $u^{\Delta,\delta}$ using the grid function u_j^n:

$$u^{\Delta,\delta}(x,t)=\sum_{n=0}^{\infty}\sum_{j=-\infty}^{\infty}u_j^n\mathbf{1}_{\mathcal{I}_j\times\mathcal{I}^n}(x,t), \tag{3.13}$$

where $\mathbf{1}_{\mathcal{I}_j\times\mathcal{I}^n}$ is the indicator function which takes value 1 when $(x,t)\in\mathcal{I}_j\times\mathcal{I}^n$, and 0 otherwise. Thus $u^{\Delta,\delta}$ depends on the grid size Δx, Δt, and the horizon parameter δ. For the continuum solution to the nonlocal model, we use the notation u^δ to explicitly emphasize the dependence on δ. it is shown in [1] that

(i) for a fixed $\delta > 0$, with Δx to 0, $u^{\Delta,\delta}$ converges to the entropy solution u^δ of the nonlocal conservation law (1.1) in $L^1_{\rm loc}(\mathbb{R})$ uniformly for $t \in [0,T]$. More precisely,

$$\lim_{\Delta x\to 0}\sup_{t\in[0,T]}\int_{\mathbb{R}}|u^{\Delta,\delta}(\cdot,t)u^{\delta}(\cdot,t)|\mathrm{d}x\mathrm{d}t=0; \tag{3.14}$$

(ii) as δ and Δx both go to 0, $u^{\Delta,\delta}$ converges to the entropy solution of local conservation law (1.2), $u^{\rm local}:[0,T]\to L^1(\mathbb{R})$, in $L^1_{\rm loc}(\mathbb{R})$ uniformly for $t\in[0,T]$. More precisely,

$$\lim_{(\Delta x,\delta)\to(0,0)}\sup_{t\in[0,T]}\int_{\mathbb{R}}|u^{\Delta,\delta}(\cdot,t)-u^{\rm local}(\cdot,t)|\mathrm{d}x\mathrm{d}t=0. \tag{3.15}$$

4. Numerical experiments

In this section, we will perform numerical experiments on scheme (3.1) for our nonlocal conservation law (1.1). We will pick g as the Godunov flux function corresponding to the finite difference scheme of the classical Burgers' equation (1.2).

We will perform five groups of numerical experiments for the nonlocal scheme (3.1), each with different initial data u_0 and kernels ω^δ:

(i) fix δ and refine Δx. The numerical solution of nonlocal Burgers' equation converges;

(ii) fix Δx and refine δ. The numerical solution of nonlocal Burgers' equation converges to the numerical solution of local Burgers' equation;

(iii) fix the number of interaction cells, $r=\lfloor\delta/\Delta x\rfloor$, and refine both δ and Δx at the same time. The numerical solution of nonlocal Burgers' equation converges to the entropy solution of local Burgers' equation.

4.1. Set up g, u_0 and ω^δ

We will take g as the Godunov flux g^G for the finite difference scheme of the classical Burgers' equation $u_t+uu_x=0$:

$$g^G(u_j^n,u_{j+1}^n)=\begin{cases}\min\limits_{u_j^n\le\theta\le u_{j+1}^n}\theta^2/2, & \text{if } u_j^n\le u_{j+1}^n,\\ \max\limits_{u_{j+1}^n\le\theta\le u_j^n}\theta^2/2, & \text{if } u_j^n\ge u_{j+1}^n.\end{cases}$$

Since $f(u)=u^2/2$ is strictly convex, the above formula reduces to

$$g^G(u_j^n,u_{j+1}^n)=\max\{f(\max(u_j^n,\theta^*)),f(\min(u_{j+1}^n,\theta^*))\},$$

where θ^* is the unique local minimum of f, $\theta^*=0$. That is,

$$g^G(a,b)=\frac{1}{2}\max\{(a^+)^2,(b^-)^2\}. \tag{4.1}$$

For the nonlocal interaction kernel ω^δ, we focus on kernels that are power-like functions. Let $p>-1$, consider the following density function ρ, and the corresponding kernel $\omega^\delta(h)=\rho(h/\delta)/\delta$:

$$\rho(h)=(1+p)h^p\mathbf{1}_{(0,1)}(h),\quad \omega^\delta(h)=\big(\frac{1+p}{\delta^{1+p}}\big)h^p\mathbf{1}_{(0,\delta)}(h). \tag{4.2}$$

In the reported experiments, we use three initial conditions, all are periodic with respect to the $[-1,1]$. The first two initial conditions are piecewise-constant functions for Riemann problem, while the third is a smooth function:

$$u_0^1(x) = \begin{cases} 1, & x \in [-1,0), \\ 0, & x \in [0,1]; \end{cases}, \quad u_0^2(x) = \begin{cases} -1, & x \in [-1,0), \\ 1, & x \in [0,1]; \end{cases}, \quad u_0^3(x) = \sin \pi x.$$

The initial data u_j^0 in the discrete level is taken as the cell average given in (3.1).

Remark 4.1 (1) In our experiments, we investigate how the following elements would affect the numerical solutions: time T, horizon δ, grid-size Δx, initial data u_0^i, and p, the power parameter that determines kernel ω^δ in (4.2).

(2) In all experiments we fix $\frac{\Delta t}{\Delta x} = 0.25$, which makes nonlocal CFL condition (3.12) hold, for g^G and all $p > -1$.

(3) We only consider the case when δ is a multiple of cell size Δx, such that $r = \lfloor \delta/\Delta x \rfloor$ is a nonnegative integer.

(4) In all our plots, black curve represents the initial data.

4.2. Experiment 1: fix δ, refine Δx

In Figure 1, we fix horizon $\delta = 0.2$, terminal time $T = 0.6$, and refine Δx.

Columns of Figure 1 correspond to different choices of initial data u_0^i, while the rows indicate different p values. In each plot, the color blue, cyan, green, yellow, purple and red correspond to $\Delta x = \frac{1}{8}$, $\frac{1}{16}$, $\frac{1}{32}$, $\frac{1}{64}$, $\frac{1}{128}$ and $\frac{1}{256}$, respectively. The plots show that, as we refine Δx, the curves get closer and appear to converge.

Error $\|u^{\Delta,\delta} - u^\delta\|$, kernel ω_1^δ, $p = 1$			
dx	L^1	L^∞	BV
1/8	0.1929	0.5619	1.3261
1/16	0.0944	0.3125	0.7579
1/32	0.0458	0.1983	0.4721
1/64	0.0214	0.1120	0.2634
1/128	0.0093	0.0539	0.1261
1/256	0.0031	0.0196	0.0455

Table 1 Errors between nonlocal numerical solutions and nonlocal "true" solution, with $p = 1$, $\delta = 0.2$, $T = 0.6$

It is also interesting to observe how the p value impacts the nonlocal solutions under the same δ at the same time T. In general, the smaller p is, the more the nonlocal solutions look like the solution of local Burgers' equation. More specifically, for u_0^1, when p decreases from 1 to -0.9, the discontinuity introduced by u_0^1 flats out less, and the nonlocal solution appears steeper near $x = 0.3$. While in the u_0^2 case, we see the opposite. As p decreases, the discontinuity in the

nonlocal solution flats out faster, and the nonlocal solution appears smoother near $x = 0$. For the smooth initial data u_0^3, the smaller p is, the more nonlocal solution looks more like a shock, a matter that will be investigated further in our future works.

Error $\|u^{\Delta,\delta} - u^{\delta}\|$, kernel ω_2^{δ}, $p = 0$			
dx	L^1	L^∞	BV
1/8	0.1899	0.5261	1.2469
1/16	0.0963	0.3750	0.8666
1/32	0.0467	0.2779	0.6196
1/64	0.0220	0.1848	0.4039
1/128	0.0096	0.1041	0.2252
1/256	0.0032	0.0439	0.0939

Table 2 Errors between nonlocal numerical solutions and nonlocal "true" solution, with $p = 0$, $\delta = 0.2$, $T = 0.6$

Error $\|u^{\Delta,\delta} - u^{\delta}\|$, kernel ω_3^{δ}, $p = -0.9$			
dx	L^1	L^∞	BV
1/8	0.1469	0.2906	0.8621
1/16	0.0787	0.2943	0.7463
1/32	0.0393	0.2786	0.6307
1/64	0.0188	0.2637	0.5612
1/128	0.0084	0.2484	0.5119
1/256	0.0031	0.2275	0.4600

Table 3 Errors between nonlocal numerical solutions and nonlocal "true" solution, with $p = -0.9$, $\delta = 0.2$, $T = 0.6$

Error $\|u^{\Delta,\delta} - u^{\Delta,0}\|$ with $p = 0$			
δ	L^1	L^∞	BV
0.32	0.1237	0.1436	0.7929
0.16	0.0682	0.0821	0.6251
0.08	0.0394	0.0894	0.5139
0.04	0.0212	0.0721	0.3246
0.02	0.0122	0.0489	0.1742
0.01	0.0096	0.0357	0.1039

Table 4 Errors between nonlocal numerical solutions and local true solution, with $p = 0$

Tables 1–3 list the errors of numerical solutions in L^1, L^∞ and BV norms, for $p = 1$, $p = 0$ and $p = -0.9$, respectively, with the smooth initial dat u_0^3. Again, $\delta = 0.2$ and $T = 0.6$ are used. The "true" nonlocal solution u^{δ} is taken as a solution computed on a sufficiently fine mesh, with

$\Delta x = \frac{1}{512}$ and $\Delta t = \frac{\Delta x}{4}$. The tables show that, as we refine Δx, the errors are decreasing, no matter which norm is used. For the $p = -0.9$ case, the L^∞ and BV norms do not reduce as significantly as the $p = 1$ and $p = 0$ case. It may be due to possible shock formation near $x = 0$ when $p = -0.9$ as mentioned above.

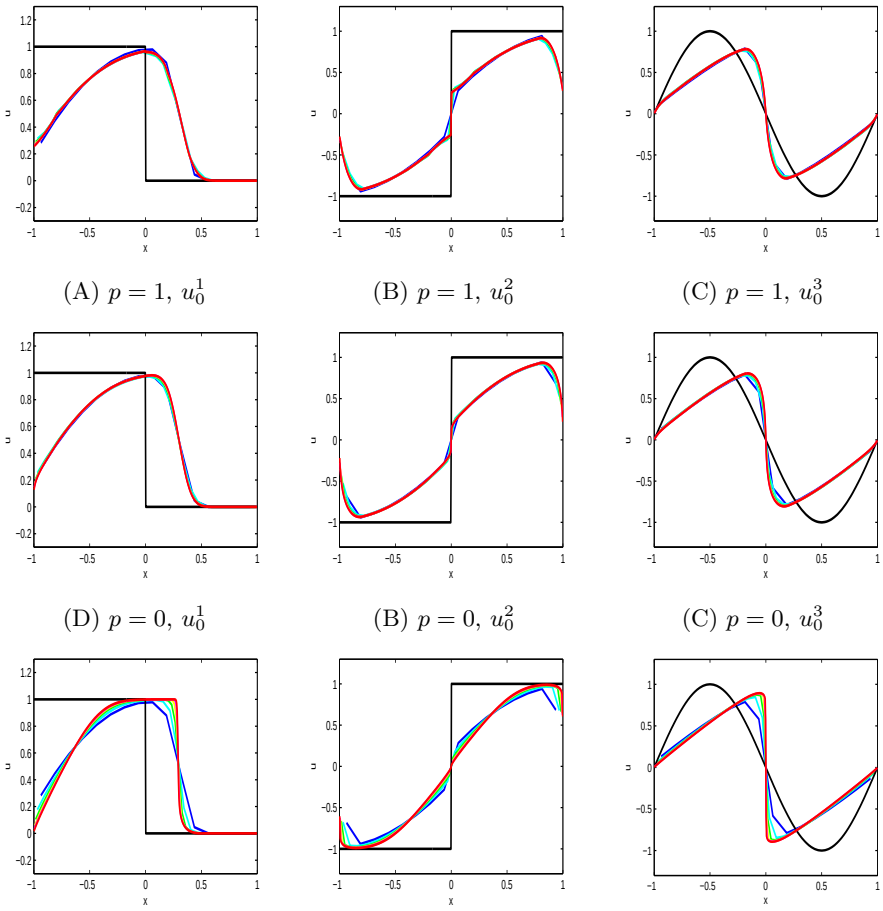

(A) $p = 1$, u_0^1 (B) $p = 1$, u_0^2 (C) $p = 1$, u_0^3

(D) $p = 0$, u_0^1 (B) $p = 0$, u_0^2 (C) $p = 0$, u_0^3

(G) $p = -0.9$, u_0^1 (H) $p = -0.9$, u_0^2 (I) $p = -0.9$, u_0^3

Figure 1 Solutions for $\delta = 0.2$, $T = 0.6$ and decreasing Δx. The colors blue, cyan, green, yellow, purple and red correspond to $\Delta x = \frac{1}{8}$, $\frac{1}{16}$, $\frac{1}{32}$, $\frac{1}{64}$, $\frac{1}{128}$ and $\frac{1}{256}$, respectively.

4.3. Experiment 2: fix Δx, refine parameter δ

In Figure 2, we fix $\Delta x = 0.005$ and $T = 0.5$ while refining δ. This means that we use a fixed spatial mesh and time steps but change the model parameter. The blue, cyan, green and purple curves correspond to solutions with respect to $\delta = 64\Delta x$, $16\Delta x$, $4\Delta x$ and Δx. From the plots we see that, as we refine δ, the curves get closer to the numerical solution, denoted by $u^{\Delta,0}$ of classical Burgers' equation on the same mesh. Tables 4–6 list the numerical errors in L^1, L^∞ and BV norms, when using $p = 0.25$, $p = 0$ and $p = -0.5$, with $T = 0.2$, $\delta = 0.2$ fixed. It is shown that, as we refine δ, the errors all decrease. Note that $u^{\Delta,0}$ is a finite difference solution

of classical Burgers' equation, and it is computed on a fine mesh of $\Delta x = \frac{1}{1600}$ and $\Delta t = \frac{\Delta x}{4}$, using the classical Godunov method.

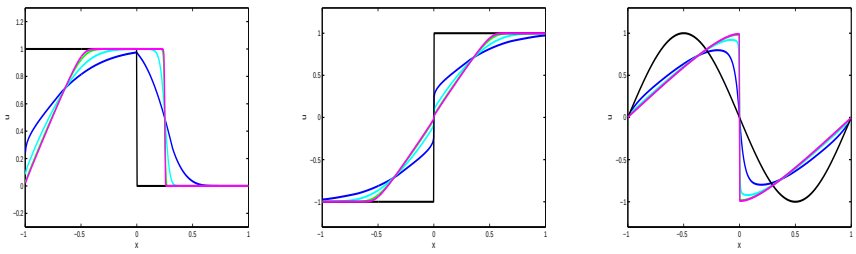

(A) $p = 0.25$, u_0^1 (B) $p = 0.25$, u_0^2 (C) $p = 0.25$, u_0^3

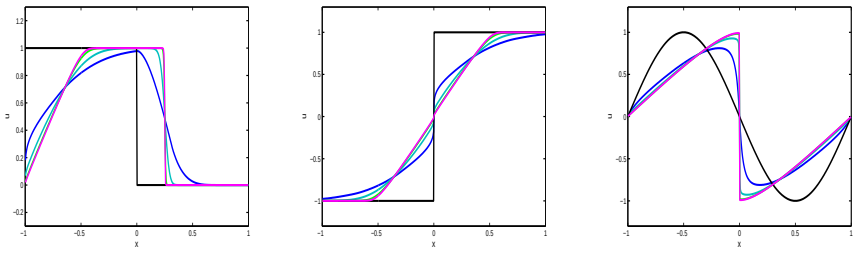

(D) $p = 0$, u_0^1 (E) $p = 0$, u_0^2 (F) $p = 0$, u_0^3

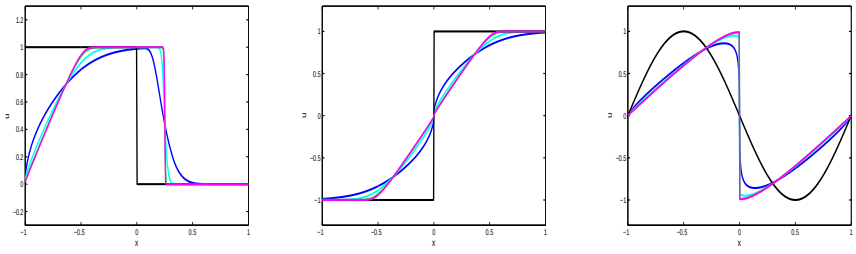

(G) $p = -0.5$, u_0^1 (H) $p = -0.5$, u_0^2 (I) $p = -0.5$, u_0^3

Figure 2 Solutions with a fixed Δx and a decreasing δ

Error $\|u^{\Delta,\delta} - u^{\Delta,0}\|$ with $p = -0.5$			
δ	L^1	L^∞	BV
0.32	0.0850	0.1055	0.6007
0.16	0.0487	0.0687	0.5096
0.08	0.0280	0.0751	0.3840
0.04	0.0159	0.0587	0.2391
0.02	0.0109	0.0430	0.1418
0.01	0.0096	0.0358	0.1039

Table 5 Errors between nonlocal numerical solutions and local true solution, with $p = -0.5$

Error $\|u^{\Delta,\delta} - u^{\Delta,0}\|$ with $p = 0.25$			
δ	L^1	L^∞	BV
0.32	0.1371	0.1563	0.8691
0.16	0.0750	0.0904	0.6578
0.08	0.0439	0.0965	0.5605
0.04	0.0240	0.0808	0.3656
0.02	0.0138	0.0558	0.1999
0.01	0.0108	0.0404	0.1172

Table 6 Errors between nonlocal numerical solutions and local true solution, with $p = 0.25$

4.4. Experiment 3: fix r, refine both Δx and δ simultaneously

In Figures 3–5, we again use $p = 0.25$, $p = 0$ and $p = -0.5$, respectively. In each case, we fix $r = 2$ and $r = 5$ while refining δ and Δx by half each time. The blue, cyan, green, purple and red colored curves correspond to $\delta = 0.2$, 0.1, 0.05, 0.025 and 0.0125 at $T = 0.5$.

As the plots show, for all three initial data u_0^i and p, no matter what value r takes on, as δ and Δx are refined at the same time, the nonlocal numerical solutions get closer to the corresponding finite difference solution of classical Burgers' equation.

Also, if we compare the plots with the same r but different p values, we observe similar phenomenon as Experiment 1: when p decreases, the more the nonlocal solutions look like the solution of local Burgers' equation.

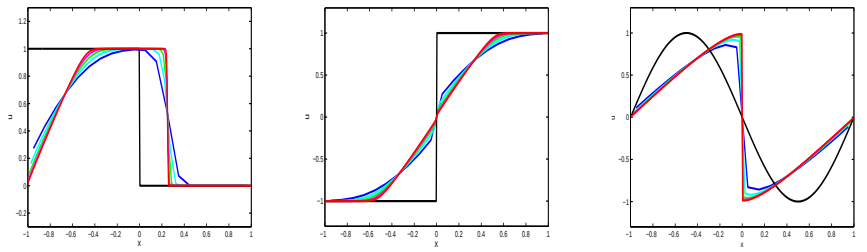

(A) $r = 2$, u_0^1 (B) $r = 2$, u_0^2 (C) $r = 2$, u_0^3

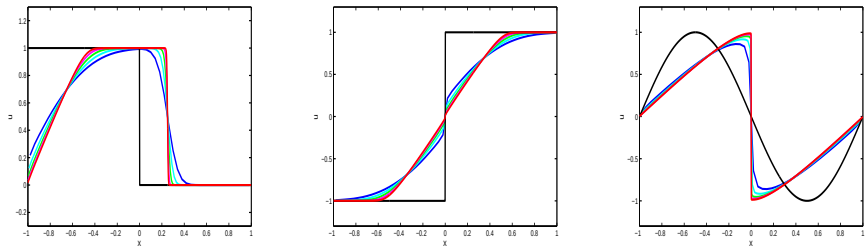

(D) $r = 5$, u_0^1 (E) $r = 5$, u_0^2 (F) $r = 5$, u_0^3

Figure 3 Solutions for $p = 0.25$, with a fixed r and decreasing Δx

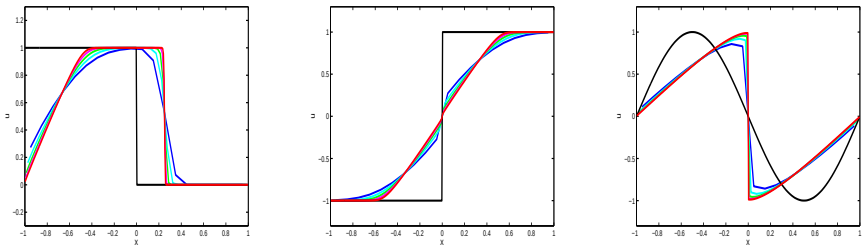

(A) $r = 2$, u_0^1 (B) $r = 2$, u_0^2 (C) $r = 2$, u_0^3

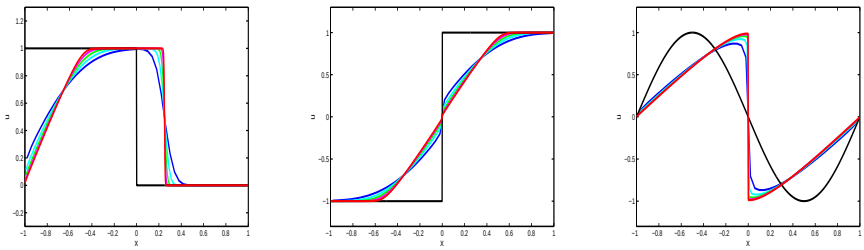

(D) $r = 5$, u_0^1 (E) $r = 5$, u_0^2 (F) $r = 5$, u_0^3

Figure 4 Solutions for $p = 0$, with a fixed r and decreasing Δx

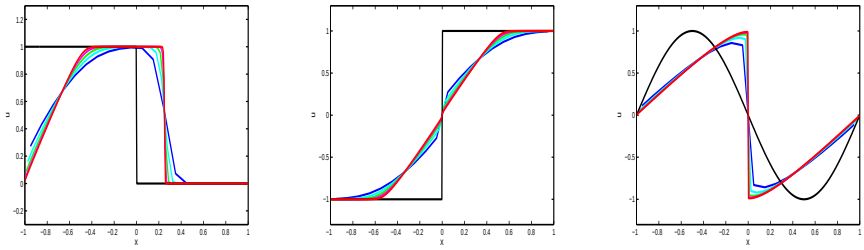

(A) $r = 2$, u_0^1 (B) $r = 2$, u_0^2 (C) $r = 2$, u_0^3

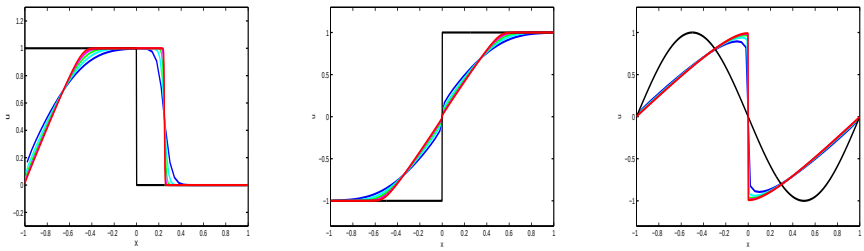

(D) $r = 5$, u_0^1 (E) $r = 5$, u_0^2 (F) $r = 5$, u_0^3

Figure 5 Solutions for $p = -0.5$, with a fixed r and decreasing Δx

5. Summary and future work

We studied a recently proposed nonlocal conservation laws that may be represented as a reasonable generalization of the local conservation law. By adopting a monotone scheme, we see

that computationally, the numerical solutions for a given horizon δ converge, as $\Delta x \to 0$, to the entropy solution of the nonlocal conservation law, while as both δ and Δx vanish, the numerical solutions converge to the entropy solution of the local conservation law. These experimental results are consistent with the theoretical findings established in [1].

There are several directions that may deserve further exploration:

• The regularity of the solutions of nonlinear nonlocal conservation laws. One of the most intriguing features of the nonlinear local conservation laws is about shock formation. We see numerical evidence of similar phenomena for the nonlocal models and we will report further theoretical analysis elsewhere.

• Higher order scheme. In the local case, the accuracy order of a monotone scheme is at most 1. For our nonlocal monotone scheme (3.1), Experiment 2 suggests that its accuracy order is also no larger than 1. It would be interesting to explore higher-order numerical schemes.

• Nonlocal-in-time. The nonlocality in our nonlocal conservation law is focused on the spacial variable. We could also try to non-localize the time variable, similar to the study given in [30] for linear nonlocal-in-time diffusion models.

• Higher dimensional problems and systems. Our work has focused on a scalar u with $x \in \mathbb{R}$. There are many open questions when u is a vector-valued function defined in multidimensional space. Such generalizations will surely be of more interests in many applications.

References

[1] Qiang DU, Zhan HUANG, P. LEFLOCH. *Nonlocal conservation laws. I. a new class of monotonicity-preserving models.* Preprint, 2016.

[2] M. G. CRANDALL, A. MAJDA. *Monotone difference approximations for scalar conservation laws.* Math. Comp., 1980, **34**(149): 1–21.

[3] R. J. LEVEQUE. *Numerical Methods for Conservation Laws.* Second edition. Lectures in Mathematics ETH Zürich. Birkhäuser Verlag, Basel, 1992.

[4] G. ALÌ, J. K. HUNTER, D. F. PARKER. *Hamiltonian equations for scale-invariant waves.* Stud. Appl. Math., 2002, **108**(3): 305–321.

[5] P. AMORIM, R. M. COLOMBO, A. TEIXEIRA. *On the numerical integration of scalar nonlocal conservation laws.* ESAIM Math. Model. Numer. Anal., 2015, **49**(1): 19–37.

[6] H. BAE, R. GRANERO-BELINCHÓN. *Global existence for some transport equations with nonlocal velocity.* Adv. Math., 2015, **269**: 197–219.

[7] S. BENZONI-GAVAGE. *Local well-posedness of nonlocal Burgers equations.* Differential Integral Equations, 2009, **22**(3-4): 303–320.

[8] A. J. J. CHMAJ. *Existence of traveling waves for the nonlocal Burgers equation.* Appl. Math. Lett., 2007, **20**(4): 439–444.

[9] S. CIFANI, E. R. JAKOBSEN. *Entropy solution theory for fractional degenerate convection-diffusion equations.* Ann. Inst. H. PoincaréAnal. Non Linéaire, 2011, **28**(3): 413–441.

[10] Renjun DUAN, K. FELLNER, Changjiang ZHU. *Energy method for multi-dimensional balance laws with non-local dissipation.* J. Math. Pures Appl. (9), 2010, **93**(6): 572–598.

[11] F. KISSLING, P. G. LEFLOCH, C. ROHDE. *A kinetic decomposition for singular limits of non-local conservation laws.* J. Differential Equations, 2009, **247**(12): 3338–3356.

[12] Hailiang LIU. *Wave breaking in a class of nonlocal dispersive wave equations.* J. Nonlinear Math. Phys., 2006, **13**(3): 441–466.

[13] M. M. MEERSCHAERT, A. B. DAVID, B. BORIS. *Multidimensional advection and fractional dispersion.* Phys. Rev. E, 1999, **59**(5): 5026.

[14] P. MIŠKINIS. *Some properties of fractional Burgers equation.* Math. Model. Anal., 2002, **7**(1): 151–158.

[15] C. ROHDE. *Scalar conservation laws with mixed local and nonlocal diffusion-dispersion terms.* SIAM J. Math. Anal., 2005, **37**(1): 103–129.

[16] K. ZUMBRUN. *On a nonlocal dispersive equation modeling particle suspensions*. Quart. Appl. Math., 1999, **57**(3): 573–600.
[17] F. ANDREU-VAILLO, J. M. MAZÓN, J. D. ROSSI, J. TOLEDO-MELEROET. *Nonlocal diffusion problems*. Mathematical Surveys and Monographs, 165. American Mathematical Society, Providence, RI; Real Sociedad Matemática Española, Madrid, 2010.
[18] L. V. IGNAT, J. D. ROSSI. *A nonlocal convection-diffusion equation*. J. Funct. Anal., 2007, **251**(2): 399–437.
[19] Qiang DU, Zhan HUANG, R. B. LEHOUCQ. *Nonlocal convection-diffusion volume-constrained problems and jump processes*. Discrete Contin. Dyn. Syst. Ser. B, 2014, **19**(4): 961–977.
[20] Tian HAO, Lili JU, Qiang DU. *Nonlocal convection-diffusion problems and finite element approximations*. Comput. Methods Appl. Mech. Engrg., 2015, **289**: 60–78.
[21] Qiang DU, J. R. KAMM, R. B. LEHOUCQ, M. L. PARKS. *A new approach for a nonlocal, nonlinear conservation law*. SIAM J. Appl. Math., 2012, **72**(1): 464–487.
[22] S. K. GODUNOV. *A difference method for numerical calculation of discontinuous solutions of the equations of hydrodynamics*. Mat. Sb. (N.S.), 1959, **47**(89): 271–306. (in Russian)
[24] S. A. SILLING, R. B. LEHOUCQ. *Peridynamic theory of solid mechanics*. Advances in Applied Mechanics, 2010, **44**(1): 73–166.
[23] S. A. SILLING. *Reformulation of elasticity theory for discontinuities and long-range forces*. J. Mech. Phys. Solids, 2000, **48**(1): 175–209.
[25] Qiang DU, M. GUNZBURGER, R. B. LEHOUCQ, Kun ZHOU. *Analysis and approximation of nonlocal diffusion problems with volume constraints*. SIAM Rev., 2012, **54**(4): 667–696.
[26] Qiang DU, M. GUNZBURGER, R. B. LEHOUCQ, Kun ZHOU. *A nonlocal vector calculus, nonlocal volume-constrained problems, and nonlocal balance laws*. Math. Models Methods Appl. Sci., 2013, **23**(3): 493–540.
[27] Xiaochuan TIAN, Qiang DU. *Asymptotically compatible schemes and applications to robust discretization of nonlocal models*. SIAM J. Numer. Anal., 2014, **52**(4): 1641–1665.
[28] Kun ZHOU, Qiang DU. *Mathematical and numerical analysis of linear peridynamic models with nonlocal boundary conditions*. SIAM J. Numer. Anal., 2010, **48**(5): 1759–1780.
[29] Xiaochuan TIAN, Qiang DU. *Analysis and comparison of different approximations to nonlocal diffusion and linear peridynamic equations*. SIAM J. Numer. Anal., 2013, **51**(6): 3458–3482.
[30] Qiang DU, Jiang YANG, Zhi ZHOU. *Analysis of a nonlocal-in-time parabolic equation*. Disc Cont Dyn Sys B, 2017, **22**: 339–368.
[31] L. J. DAVID. *Nonlocal advection equations*. International Journal of Mathematical Education in Science and Technology, 2003, **34**(2): 271–277.